J. Plasma Fusion Res. SERIES, Vol. 5 (2002) 69–76

Divertor Requirements and Performance in ITER

SUGIHARA Masayoshi
ITER International Team, Naka-machi, Naka-gun, Ibaraki, 311-0193, Japan

(Received: 11 December 2001 / Accepted: 17 May 2002)

Abstract

A variety of functions required for the ITER divertor are (i) heat removal, (ii) fuel density control, (iii) exhaust of helium ash and other impurities, (iv) providing proper magnetic configuration for enhanced confinement (H-mode). These requirements are shown to be satisfied in ITER by the sophisticated numerical code for divertor (B2-EIRENE) validated with various experimental databases. More work is necessary for the development of a pedestal model, transport in the SOL region and separatrix density, which somewhat influence the divertor solutions. Analysis based on numerical code calculation shows that core fuelling is necessary to form the density pedestal required in ITER, which is equipped with high field side pellet fuelling for this purpose. Transient large heat load during Type-I ELM activity could cause large erosion of the divertor plate, though the proposed ELM models and the database still need further improvement and development. Further inclination of the divertor target plate can mitigate the effect of ELM energy load. The discharge regime with small ELMs and high pedestal pressure (Type II ELM) can be used for hybrid and steady-state modes of operation. The inductive high Q mode can also be operated with Type II ELMs with reduced plasma current and fusion power, though its operation window is narrow. Further improvement of confinement with low density and/or higher q_{95} can widen the window significantly.

Keywords:
tokamak, divertor, SOL, pedestal, H-mode, ELM, ITER

1. Introduction

The major mission of ITER (International Thermonuclear Experimental Reactor) is to achieve 400MW of fusion power with Q=10 for several hundred seconds by inductive current drive [1]. In addition, steady state operation with $Q\approx5$ by non-inductive current drive is to be aimed at. Reasonable operation windows for these operation scenarios are indispensable to accomplish the overall missions of ITER. To achieve these missions, relevant plasma performance is required which is highly dependent on the divertor performance, e.g., radiative cooling, helium ash exhaust and impurity control. The divertor performance must also be compatible with the engineering requirements, e.g., heat removal capability, DT particle throughput and core fuelling capability.

The requirement of heat removal must be satisfied both during steady and transient conditions. During steady conditions, the peak heat flux density must be below an engineering limit. Heat removal during Type I ELMs is a main issue during transient conditions. Energy loss during Type I ELMs is correlated with high pedestal pressure, which is required for good energy confinement, and consequently, the heat load could be severe. It is therefore of primary importance to predict the energy loss during ELMs in ITER by predictive models or scalings based on the ELM database. Development of mitigation methods of the ELM effect must also be carried out in parallel with the

Corresponding author's e-mail: sugiham@itergps.jaeri.go.jp

Table 1 Divertor requirements in ITER.

Requirements	
1. Peak power load on the target plates (q_{pk})	$q_{pk} \leq 10$ MW/m^2
2. Helium concentration in the core plasma (C_{He})	$C_{He} \leq 0.06$
3. Z_{eff} in the core plasma	$Z_{eff} \leq 1.6$
4. Upstream plasma density (n_s)	$n_s \leq 0.33\times10^{20}$ m^{-3}
5. D-T particle throughput (Γ_{DT})	$\Gamma_{DT} \leq 200$ Pa·m^3/s
6. Core fuelling (Γ_{DT}^{core})	0 £ $\Gamma_{DT}^{core} \leq 100$ Pa·m^{3}s^{-1}

development and improvement of these predictive models and database.

In this paper, the required divertor functions for core plasma performance and the divertor's engineering constraints are summarised in Sec. **2**. In Sec. **3**, divertor performances are examined using the sophisticated numerical code B2/Eirene. In Sec. **4**, the remaining uncertainties and further necessary development of the models are briefly reviewed. In Sec. **5**, the effects of Type I ELMs are examined and a prediction of ITER case is performed using proposed models. The uncertainties of each models and database are discussed. Possible mitigation methods and future R&D which is necessary are also presented.

2. Required divertor performances

A variety of functions are required for the divertor in ITER. Major functions required are (1) heat removal, (2) fuel density control, (3) exhaust of helium ash and impurity control, (4) provision of a proper magnetic configuration for enhanced confinement (H-mode). More specifically, the requirements can be summarised in Table 1. Those six requirements must be simultaneously satisfied. On the other hand, since the core plasma and SOL/divertor plasma are closely linked through the H-mode edge transport barrier region (pedestal region), the required divertor performances must be satisfied consistently with the core plasma parameters. Schematics of these links are shown in Fig. 1. The average temperature in the core plasma strongly depends on the pedestal temperature due to the profile stiffness and the average density is very close to the pedestal density due to the expected flat density profile. The pedestal density is closely linked with the separatrix density through the fuelling scheme and the transport characteristics of the barrier region. Divertor performance strongly depends on the separatrix density and transport in the SOL region, which is smoothly connected to the pedestal region where transport is

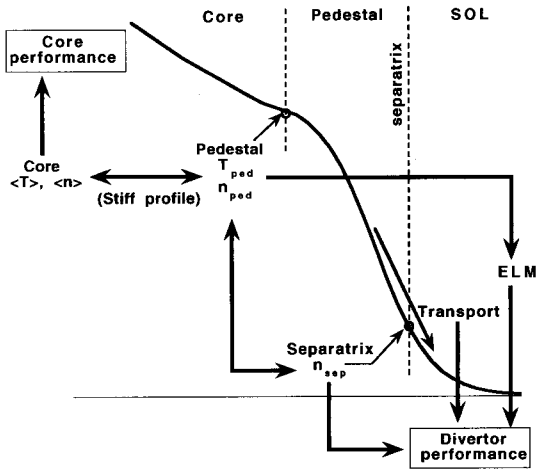

Fig. 1 Schematics of the links between core plasma and divertor plasma through a pedestal.

governed by the characteristics of the critical pressure gradient due to the ideal ballooning mode for the Type-I ELMy discharge regime (ITER's reference operation regime). High pedestal pressure required for good energy confinement of the core plasma can result in high energy deposition during Type-I ELMs on the divertor plate [2], which can have a large impact on the divertor life time as well as on the impurity generation from the divertor plate.

Other constraints are the engineering limits, such as peak heat flux on the divertor plate, DT particle throughput due to the tritium inventory limitation, core fuelling due to the limitation of the particle injection technique, and pumping speed. The upper limit of the DT particle throughput and the core fuelling rate are requirements, but at the same time, these are control actuators. The numbers of actuators are not so many and they are; (i) Divertor geometry, (ii) DT particle throughput, (iii) Core fuelling, (iv) Pumping speed and (v) Impurity seeding (Neon, Argon and others). Divertor geometry is not a real time actuator but is fairly

important to supplement the controllability of the divertor with small numbers of actuators. Actuators (ii), (iii) and (iv) can control the separatrix density n_s to some extent, and the helium concentration as well as the peak heat flux can be controlled through n_s as shown later.

3. Predicted divertor performances

The divertor performance of ITER has been examined and optimised using a sophisticated numerical code B2/Eirene, which has been validated against various experimental results in ASDEX-U, JET and JT-60U. Details of the code and model validation are published elsewhere [3,4]. Major assumptions for the examinations and optimisations of ITER are summarised as follows;

- Transport coefficients; D=0.3 m^2/s, χ=1 m^2/s, no parameter dependence and spatially constant both in SOL and pedestal regions,
- The effect of ELMs is time averaged (not included explicitly),
- Carbon sputtering (physical and chemical) is properly included, while they are assumed to be absorbed at every surface encountered.
- The divertor plasma is optimised in a partially detached condition.

First, optimisation of divertor geometry has been extensively performed. It is found that the enhancement of neutral accumulation in the divertor region, in particular, near the separatrix region of the outer target plate, is essential for the reduction of peak heat load. Long divertor length, vertically inclined divertor plate and installation of the divertor dome are effective for this purpose and have been employed from the initial phase of ITER design as a basic divertor structure. Later, more sophisticated refinements of the geometry are performed after detailed numerical investigations. The first refinement is a modification of the bottom part of the divertor near the strike point of the outer plate from a straight-shape to a V-shape configuration as shown in Fig. 2. With this refinement, it is expected that neutral particles accumulate more near the separatrix and accelerate the partial detachment of plasma in this region, where the heat load is highest. JET demonstrated this effect experimentally [5]. In fact, the divertor code calculation for ITER shows that peak heat load can be reduced by about 30 % with this refinement. The second refinement is a modification of the support structure of the divertor dome to permit neutral gas circulation between the inner and outer divertor. It is widely

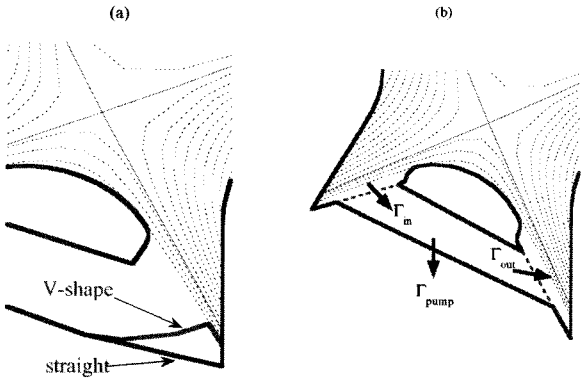

Fig. 2 (a) V-shape and straight bottom plate of divertor. (b) Connection of inner and outer divertor region to allow neutral flow from inner to outer.

recognised experimentally and numerically that particle flux is higher at the inner divertor target than the outer and the other way around for the heat flux. For this reason, detachment of the inner is easier. By connecting the inner and the outer divertor region, neutrals can flow from the inner to the outer and neutral accumulation near the separatrix of the outer divertor can be increased. This feature has been confirmed by JET [6] and JT-60U experiments [7]. An ITER calculation has been done by changing the probability for neutrals to flow from the inner to the outer. The actual ITER design corresponds to a probability of 0.56 (170–220 Pa·m^3/s) and the peak heat load can be reduced by about 20 % compared with the case of no gas flow between the inner and the outer divertor regions.

The upstream separatrix density n_s has a dominant effect on divertor performance. With increasing n_s, the peak heat flux can be substantially reduced. However, n_s must be within the range consistent with high energy confinement during H-mode. On the other hand, n_s can be controlled by gas-puffing and/or core fuelling (throughput Γ_{DT}) to some extent. The controllable range of n_s is actually rather narrow ($0.27 \leq n_s(10^{20}) \leq 0.32$ for $70 \leq \Gamma_{DT}$(Pa·m^3/s) ≤ 200 and P_{SOL}(power across separatrix)=86 MW). With increasing P_{SOL}, n_s increases while the controllable range is relatively unchanged.

Based on the detailed examinations and optimisations for divertor performance described above, representative scenarios for inductive and steady state operation of ITER are investigated [8]. Major parameters for the reference operation modes are summarised in Table 2. For the reference inductive operation mode, the peak heat load q_{pk} decreases from 10 MW/m^2 to 4 MW/m^2 when the DT particle

Table 2 Major parameters for inductive and steady-state operation scenarios in ITER.

	Inductive operation	Steady-state operation
Plasma major / minor radius (m)	6.2 / 2	6.2 / 2
Elongation κ_{95} / triangularity δ_{95}	1.7 / 0.33	1.7 / 0.33
Plasma current (MA) / Toroidal field (T)	15 / 5.3	10 / 5.3
Safety factor q_{95}	3	4.5
Fusion power (MW)	410	340
Total heating power P_{Total} (MW)	123	128
Power across separatrix P_{SOL} (MW)	86	100
Q value	10	5.7
Average density $\bar{n}_e$ (10^{20} m^{-3})	1.01	≈ 0.7

throughput Γ_{DT} is changed from 70 to 180 Pa·m^3/s (correspondingly n_s is changed from 0.27 to 0.32 × 10^{20} m^{-3}, which is within the requirement) for fixed pumping speed (20 m^3/s). The helium concentration C_{He} also decreases with this increase of Γ_{DT} from 5 to 2 % due to the increased helium exhaust efficiency with increased neutral compression. Other series of calculation results with increased fusion power and pumping speed show that the fusion power (helium source) and Γ_{DT} dominate the helium concentration, while the pumping speed is less important.

For the reference steady state operation mode, operation density must be reduced, which increases the peak heat load. On the other hand, connection length becomes longer due to decreased plasma current or increased q_{95}, which compensates the reduction of density to some extent. Calculation results show that q_{pk}=10 MW/m^2 is reached at $n_s \approx 0.26 \times 10^{20}$ m^{-3}, which is slightly higher than the requirement of $\bar{n}_e/3$=0.23×10^{20} m^{-3}. In spite of relatively low n_s, helium concentration stays low due to lower fusion power. To further reduce the peak heat load within the requirement of n_s, initial study of impurity seeding is performed. With 0.4 % of neon seeding, ≈30 % reduction of q_{pk} is achieved while increase of effective charge ΔZ_{eff}≈0.4 (total Z_{eff}≈1.6) is marginally acceptable.

4. Further model development needed and remaining uncertainty

Although extensive model validations have been done for the B2/Eirene code, there still remains some uncertainty, and further model development is necessary in some areas.

For present devices, the appropriate density pedestal can be reproduced by the code with the assumed diffusion coefficient, since significant amount

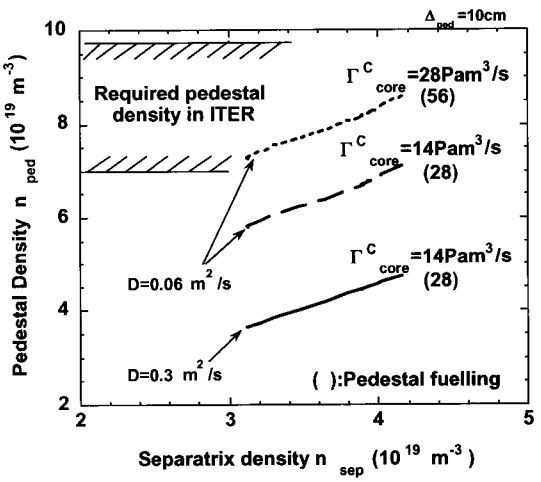

Fig. 3 Pedestal density evaluated for diffusion coefficients in the pedestal region D=0.3 and 0.06m^2/s and for different core fuelling Γ^C_{core}=14 and 28Pa·m^3/s. The corresponding required pedestal fuellings are shown in parentheses.

of neutral particles can penetrate inside the pedestal region due to narrow SOL thickness. However, if only gas-puffing is used, high pedestal density (n_{ped}≈10^{20} m^{-3}) cannot be achieved even if the diffusion coefficient is neo-classical level (0.06 m^2/s), since only a small fraction of gas-puffed neutrals can penetrate across the separatrix due to thick SOL in ITER. This indicates a need for core fuelling. Relation between the separatrix density and the pedestal density can be approximately expressed as

$$n_{ped} = n_s + \Gamma^C_{core}\Delta_{ped}/SD \quad (1)$$

where Γ^C_{core}, Δ_{ped} and S are core fuelling rate, pedestal width and plasma surface area, respectively. Here, the particle pinch term is omitted for simplicity. Fig. 3 shows the achievable pedestal density for the present

Table 3 Allowable energy density during ELMs and the energy loss fraction with respect to pedestal stored energy for CFC and tungsten divertor plate in ITER. 10^6 ELM events and 100MJ of pedestal stored energy are assumed.

	CFC	W
Allowable $\Delta W_{ELM}/S_{ELM}$ (MJ / m^2) for 10^6 ELM events* (≈1000 shots)	0.55	0.72
Allowable $\Delta W_{ELM}/W_{ped}$ (%) for 10^6 ELM events with deposition area $S_{ELM} \approx 2 \times S_{ss} \approx 6 - 15$m^2 $W_{ped} \approx 100$MJ	3.4 – 8.6	4.4 – 11

divertor model calculation (solid line), reduced diffusion coefficient with core fuelling rate of 14 Pa·m^3/s (dashed line) and 28 Pa·m^3/s (dotted line), respectively. Δ_{ped} is assumed to be 10cm [9]. Here, core fuelling denotes the particle injection inside the transport barrier region. Injection of particles within the pedestal region (pedestal fuelling) can also achieve the pedestal density required for ITER, while, in this case, the efficiency of density increase is lower compared with core fuelling. A rough estimation of the fuelling for this case is shown in the bracket. High field side pellet injection (50–100 Pa·m^3/s and deposition depth=0.15a with 500 m/s) is foreseen for ITER so that these core fuelling requirements can be met. Divertor performance is dominantly determined by n_s and power flow across the separatrix. Therefore, the divertor solutions presented in this paper will be unchanged, even when the proper pedestal model is introduced, as long as n_s is kept in a similar range.

Other uncertainties remaining in this divertor model are the assumed transport coefficients in the SOL region and an acceptable range of separatrix density for good H-mode confinement. Further database archive and data examinations in these issues are being carried out as part of the ITPA (International Tokamak Physics Activity) by the Divertor/SOL physics Topical Group.

5. ELM effects and mitigation

High pedestal pressure required for good H-mode confinement can result in large divertor erosion due to Type-I ELMs, which is the reference ITER operation mode for the $Q \geq 10$ inductive scenario. Criteria for the allowable energy loss due to ELMs can be expressed as

$$\Delta W_{ELM} / (S_{ELM} \sqrt{\tau_{ELM}}) \quad (2)$$

which is a measure for surface temperature rise of the target. Here ΔW_{ELM}, S_{ELM}, τ_{ELM} are energy loss, deposition area and duration time for ELMs, respectively. In JET, $\tau_{ELM} \approx 200$ μs has been observed and it is rather independent of density and triangularity. There is large uncertainty in S_{ELM}. First, S_{ELM} is widened during ELMs from its width in-between ELMs S_{ss}, roughly by a factor of 2. When S_{ss} is estimated from the divertor code results, the area is rather wide due to the partial detached condition and is evaluated as ≈7.5 m^2. On the other hand, if we assume the width of heat flow becomes much narrower during ELMs due to burn-through, the width can be estimated as ≈5 mm mapped on the outer midplane, which provides $S_{ss} \approx 3$ m^2. From these assessments, the range of S_{ELM} is expected to be 6–15 m^2. Consequently, criteria for the allowable energy density $\Delta W_{ELM}/S_{ELM}$ and allowable energy loss fraction to the pedestal stored energy $\Delta W_{ELM}/W_{ped}$ for CFC (2 cm thick) and a tungsten (1cm thick) divertor plate, which can withstand 10^6 ELM events (≈1000 shots), are summarised in Table 3.

So far, several models have been proposed for summarising the experimental data $\Delta W_{ELM}/W_{ped}$. Here we will briefly review three representative models (i) collisionality ν^* model [10], (ii) parallel transport time $\tau_{\|}$ model [11] and sheath model [12] as well as their uncertainties. Common feature of all of the models is that the energy loss is closely correlated with the pedestal pressure (stored energy).

The ν^* model is based on the fact that $\Delta W_{ELM}/W_{ped}$ is simply correlated with ν^* measured at the pedestal density and temperature over wide range of ν^* (two orders of magnitude). The fitting expression is written as

$$\Delta W_{ELM} / W_{ped} = 0.064 (\nu^*)^{-0.33} \quad (3)$$

Although correlation is fairly good, the underlying physics basis must be clarified to extrapolate to ITER. One possible mechanism is that the MHD amplitude associated with ELMs is reduced with increasing density (or collisionality), which is actually observed in JET [13]. However, it is still unclear whether this reduction is attributed to the reduction of MHD amplitude itself or an increase of mode number (increased decay of MHD signal at pick-up coils). Also the mechanism as to how this

MHD amplitude relates to the actual kinetic energy loss from the pedestal must be identified. A significant loss fraction $\Delta W_{ELM}/W_{ped}$=(15–20) % is predicted for ITER ($\nu^*\approx 0.04$) when this model is applied.

The $\tau_{||}$ model is based on the assumed physics mechanism in that the pedestal region is connected to the divertor due to ergodization and the parallel energy transport along field line (characterised by $\tau_{||}$) together with the ELM duration time τ_{ELM} determine the eventual energy loss from the pedestal. Experimental data seem to be well summarised by the $\tau_{||}$ model for fixed τ_{ELM}(=200μs). The fitting expression is written as

$$\Delta W_{ELM}/W_{ped} = \frac{0.27}{1+\tau_{||}/\tau_{ELM}} \quad (4)$$

Actually, however, τ_{ELM} is different for individual machines, i.e., ≈200 μs in JET, ≈300 μs in DIII-D, ≈400 μs in ASDEX-U. When these values of τ_{ELM} are used for fitting the experimental data, the correlation becomes much worse (RMSE=0.041 compared with 0.03 with fixed τ_{ELM}=200 μs). A simple application of this model to ITER predicts a (12–15) % energy loss fraction.

The sheath model is based on the energy flux through the sheath of the divertor plate assuming that the SOL is filled with pedestal plasma parameters. The expression is written as

$$\Delta W_{ELM}/W_{ped} \propto \gamma n_{ped} c_s(T_{ped}) T_{ped} \quad (5)$$

where γ and c_s are the heat transmission coefficient and sound velocity, respectively. By nature, this model will provide the maximum available (upper limit) heat flux through the sheath when a normal sheath is formed. When compared with experimental results, the general trend is well reproduced, while the model provides higher values for ASDEX-U and DIII-D, while fairly close values to the JET data. Application of this model to ITER predicts ≈5 % for the energy loss fraction. An unresolved issue of this model is that the physics picture is somewhat contradicting the following experimental observations on $\tau_{ELM}/\tau_{||}$. When this ratio is larger than unity, the SOL is filled fairly quickly and the sheath expression is expected to be a good approximation, while in the opposite case ($\tau_{ELM}/\tau_{||}$<1), the model should overestimate the heat flux. When τ_{ELM}=300 μs (DIII-D) and τ_{ELM}=400 μs (ASDEX-U) are assumed, $\tau_{ELM}/\tau_{||}$>1 for these machines, and, thus, the model is expected to be a good approximation, while actually, it over-estimates the data. In the JET case, where $\tau_{ELM}/\tau_{||}$<1 for τ_{ELM}=200 μs, the model is expected to over-estimate, while, actually, it predicts values close to the experimental data.

From the examinations described above, it is concluded that all models are not complete and still need much more work. Although the range of model predictions and uncertainties are very large, ITER predictions are summarised in Fig. 4 when these models are simply applied to ITER. Solid lines show the allowable energy loss fraction for CFC and tungsten plate (S_{ELM}=10 m^2 is assumed) and dotted lines show the predicted loss fraction for each of these models. Dashed lines show the allowable energy loss fraction for the case of further inclined divertor plate (poloidal angle is halved from the present value 22.8° to 11.4°). Preliminary studies for engineering feasibility (alignment and assembly) show that this further inclination would be possible. Possible physical disadvantageous effects on the increased particle recycling on the upper part of the divertor plate, and modification of plasma profile around the X-point are preliminarily examined by the B2/Eirene code. Calculation results show no significant increase of particle recycling and no noticeable change of plasma profile. Another possible issue of this further inclination is that the flexibility of position control of the separatrix will be somewhat limited. This will be acceptable once the operation mode is fixed for engineering testing purposes. In fact, the life time becomes a more important issue for this testing phase. Use of a tungsten divertor plate will also be possible during this phase, since the disruption probability should be low and the melting of tungsten plate due to the disruption heat load

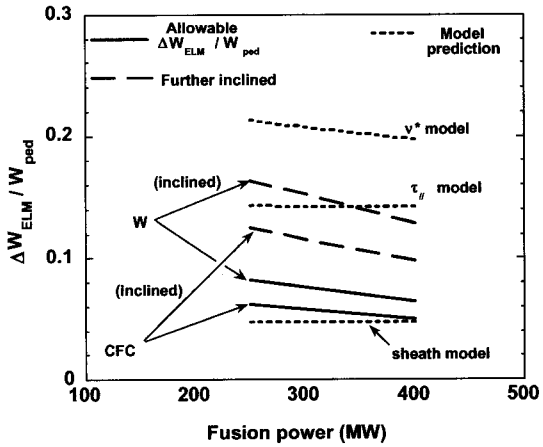

Fig. 4 Allowable energy loss fraction $\Delta W_{ELM}/W_{ped}$ for CFC and tungsten (solid lines). Allowable values when the divertor plate is further inclined are also plotted (dashed lines). Values predicted by various models are plotted by dotted lines.

can be limited.

Another possible method to avoid the Type I ELM heat load is to employ the discharge regime of small ELMs with high pedestal pressure. This regime is observed in most divertor machines [14-18] and is conveniently categorised as Type II ELM, though the basic physical features may not be the same. Dominant parameters to achieve this Type II ELM regime are q_{95} and δ_x, and their ranges are typically q_{95}>3.5 – 0.4 and δ_x>0.4 – 0.5. The present ITER configuration (δ_x=0.5) satisfies the requirement for δ_x. Although the plasma current is 15 MA (q_{95}=3) in the reference ITER inductive operation mode to achieve Q=10, the operation scenario with reduced plasma current at 13 MA (q_{95}=3.5) is also possible to achieve Q=10 by reducing density ($\bar{n}/n_G$=0.7) and fusion power (≈250 MW). In this case, however, the operation window is significantly reduced. If higher confinement is achieved for higher q_{95} and/or lower density, the window becomes substantially wider. Actually, a higher HH factor has been observed with lower density for many machines and with higher q_{95}(≈3.5) with high density ($\bar{n}/n_G$≈1) in some machines [19]. Hybrid and steady state scenarios in ITER can be operated with higher q_{95}(>3.5), which facilitates the access to this small ELM Type II regime. Further R&D is needed to extend this small ELM regime with high confinement to the reference high Q inductive operation mode of ITER. Type II ELMs in-between Type I ELMs observed in JET (q_{95}=3 and δ_x=0.5) could be a clue for the R&D [13].

6. Conclusions

Various divertor requirements for ITER to achieve the specified missions within engineering constraints are summarised. Detailed studies by a sophisticated divertor code B2/Eirene show that these requirements can be satisfied with reasonable windows for inductive operation mode. For non-inductive operation mode, impurity seeding will reduce the peak heat load to meet the requirements.

Further model development is necessary for B2/Eirene to include a proper pedestal model. It is indicated that gas-puffing cannot fuel across the separatrix to form a proper density pedestal required in ITER. High field side pellet fuelling is prepared in ITER to fuel inside the pedestal. Further model validation in the area of transport in the SOL, separatrix density, impurity transport are necessary and in progress.

The effect of Type I ELM power load on the divertor could be severe for high pedestal pressure which is required for good confinement, while present predictions by proposed models are still primitive and the uncertainty of the database is large. Thus, further development and improvement of the models as well as the database are necessary.

Possible mitigation methods for Type-I ELM effects are ; further inclination of the divertor target plate and Type-II ELMs discharge regime. Hybrid and steady-state scenarios can be operated with the Type-II ELM regime with q_{95}≥3.5. Further exploration to extend this regime to high Q inductive operation mode with q_{95}=3 or further improved confinement associated with lower density or q_{95}≥3.5 should be promoted.

Acknowledgements

The author is grateful to Drs. A. Kukushkin and A. Loarte for valuable comments and discussions. The author also expresses his thanks to the members of Physics Unit of ITER International Team. This report was prepared as an account of work undertaken within the framework of ITER Co-ordinated Technical Activities (CTA). These are conducted by the Participants: Canada, the European Atomic Energy Community, Japan, and the Russian Federation, under the auspices of the International Atomic Energy Agency. The views and opinions expressed herein do not necessarily reflect those of the Participants to the CTA, the IAEA or any agency thereof. Dissemination of the information in this paper is governed by the applicable terms of the former ITER-EDA Agreement.

References

[1] Aymar, R. *et al.*, Nucl. Fusion **41**, 1301 (2001).
[2] Leonard, A.W. *et al.*, J. Nucl. Mater. **266-269**, 109 (1999).
[3] Schneider, R. *et al.*, J. Nucl. Mater. **196-198**, 810 (1992).
[4] Schneider, R. *et al.*, J. Nucl. Mater. **266-269**, 175 (1999).
[5] Monk, R. *et al.*, Proc. 24th EPS Conference on Controlled Fusion and Plasma Physics, Berchtesgaden, **21**, 117 (1997).
[6] Maggi, C.F. *et al.*, Proc. 26th EPS Conference on Controlled Fusion and Plasma Physics, Maastricht, **23J**, 201 (1999).
[7] Asakura, N. *et al.*, J. Nucl. Mater. **290-293**, 825 (2001).
[8] Kukushkin, A.S. *et al.*, Proc. 28th EPS Conference on Controlled Fusion and Plasma Physics, Madeira, Portugal, P5 105 (2001).

[9] Sugihara, M. *et al.*, Nucl. Fusion **40**, 1743 (2000).
[10] Loarte A. *et al.*, 18th IAEA Fusion Energy Conference, Sorrento, Italy (2000) IAEA-CN77/ITERP/11(R).
[11] Janeschitz, G., J. Nucl. Mater. **290-293**, 1 (2001).
[12] Shimada, M. private communications (2001).
[13] Becoulet, M., Proc. 28th EPS Conference on Controlled Fusion and Plasma Physics, Madeira, Portugal, P4 076 (2001).
[14] Ozeki, T., Chu, M.S., Lao, L.L. *et al.*, Nucl. Fusion **30**, 1425 (1990).
[15] Kamada, Y. *et al.*, Plasma Phys. Control. Fusion **38**, 1387 (1996).
[16] Greenwald, M. *et al.*, Plasma Phys. Control. Fusion **40**, A265 (2000).
[17] Stober, J. *et al.*, Plasma Phys. Control. Fusion **42**, A211 (2000).
[18] Bures, M. *et al.*, Nucl. Fusion **32**, 539 (1992).
[19] Sips, A.C.C. *et al.*, 8th IAEA TCM on H-Mode Physics and Transport Barriers, Toki, Japan, A10 (2001).